Original Article

JCBFM

Journal of Cerebral Blood Flow & Metabolism
2017, Vol. 37(8) 2833–2847
© Author(s) 2016
Reprints and permissions:
sagepub.co.uk/journalsPermissions.nav
DOI: 10.1177/0271678X16676825
journals.sagepub.com/home/jcbfm
SAGE

Non-invasive near-infrared fluorescence imaging of the neutrophil response in a mouse model of transient cerebral ischaemia

Markus Vaas[1,2], Gaby Enzmann[3], Therese Perinat[3], Ulrich Siler[4], Janine Reichenbach[4], Kai Licha[5], Anja Kipar[6], Markus Rudin[1,2,7], Britta Engelhardt[3] and Jan Klohs[1,2]

Abstract

Near-infrared fluorescence (NIRF) imaging enables non-invasive monitoring of molecular and cellular processes in live animals. Here we demonstrate the suitability of NIRF imaging to investigate the neutrophil response in the brain after transient middle cerebral artery occlusion (tMCAO). We established procedures for ex vivo fluorescent labelling of neutrophils without affecting their activation status. Adoptive transfer of labelled neutrophils in C57BL/6 mice before surgery resulted in higher fluorescence intensities over the ischaemic hemisphere in tMCAO mice with NIRF imaging when compared with controls, corroborated by ex vivo detection of labelled neutrophils using fluorescence microscopy. NIRF imaging showed that neutrophils started to accumulate immediately after tMCAO, peaking at 18 h, and were still visible until 48 h after reperfusion. Our data revealed accumulation of neutrophils also in extracranial tissue, indicating damage in the external carotid artery territory in the tMCAO model. Antibody-mediated inhibition of α4-integrins did reduce fluorescence signals at 18 and 24, but not at 48 h after reperfusion, compared with control treatment animals. Antibody treatment reduced cerebral lesion volumes by 19%. In conclusion, the non-invasive nature of NIRF imaging allows studying the dynamics of neutrophil recruitment and its modulation by targeted interventions in the mouse brain after transient experimental cerebral ischaemia.

Keywords

Cerebral ischaemia, neutrophils, mouse, near-infrared fluorescence imaging, middle cerebral artery occlusion, external carotid artery

Received 25 March 2016; Revised 31 August 2016; Accepted 25 September 2016

Introduction

Transient cerebral ischaemia is followed by an inflammatory response that has been implicated to exacerbate ischaemic injury, but also to provide the necessary environment for regeneration and repair.[1] In this regard, the role of neutrophils following cerebral ischaemia remains controversial. Histological studies have revealed recruitment of neutrophils to the ischaemic lesion in experimental models of cerebral ischaemia and patients with ischaemic stroke at time points when substantial neuronal death occurs.[2–4] Treatments that prevented vascular adhesion of neutrophils,[5,6] as well as neutropenia,[7,8] were found to result in a reduction of the ischaemic damage in preclinical studies of cerebral

[1]Institute for Biomedical Engineering, ETH & University of Zurich, Zurich, Switzerland
[2]Neuroscience Center Zurich, University of Zurich and ETH Zurich, Switzerland
[3]Theodor Kocher Institute, University of Bern, Bern, Switzerland
[4]Division of Immunology, University Children's Hospital Zurich and Children's Research Centre, Zurich, Switzerland
[5]Institute of Chemistry and Biochemistry, Freie Universität Berlin, Berlin, Germany
[6]Institute of Veterinary Pathology, University of Zurich, Zürich, Switzerland
[7]Institute of Pharmacology and Toxicology, University of Zurich, Zurich, Switzerland

Corresponding author:
Jan Klohs, Institute for Biomedical Engineering, University and ETH of Zurich, Valdimir-Prelog-Weg 4, 8093 Zurich, Switzerland.
Email: klohs@biomed.ee.ethz.ch

ischaemia. However, clinical trials using ligands or antibodies to prevent neutrophil infiltration into the brain did not show clinical benefits,[9,10] questioning the pathogenic role of neutrophils.

Neutrophils have been implicated in launching and shaping the immune response following injury. Activated neutrophils have been shown to induce superoxide production, degranulation,[11] and release specific proteases, e.g. neutrophil elastase and matrix metalloproteinase.[12,13] In addition, neutrophils interact with platelets, participate in fibrin cross-linkage and trigger thrombin activation by inducing the extrinsic tissue factor/FVIIa pathway and can thereby predispose the microvasculature to thrombosis.[14] It could therefore be hypothesized that neutrophils play key roles in cerebral ischaemia injury, mainly by exerting effects on the cerebral vasculature, but direct in vivo proof is still missing. This lack of knowledge might largely stem from the paucity of techniques that are able to specifically visualize neutrophil trafficking and function in vivo. Histological studies (e.g. myeloperoxidase staining) are often not specific for neutrophils and cannot capture the dynamic and complex (inter) actions of cells. Attempts to block neutrophil migration in vivo might have suffered from lack of specificity, i.e. other leukocyte subsets might have been blocked as well,[15] while neutrophil depletion might have caused confounding immunological side effects.[16,17]

More recently, the use of two-photon microscopy enabled the intravital tracking of neutrophils in the leptomeninges and superficial parts of the cortex of the mouse with high resolution,[18] and its application to track neutrophil in a mouse model of transient middle cerebral artery occlusion (tMCAO) has been recently shown.[19] The technique is capable to monitor local neutrophils dynamics and allows to directly observe the manipulation of cell trafficking. However, two-photon microscopy of the mouse brain requires a thinned skull region or, for assessing deeper structures, the preparation of a cranial window, which may lead to immediate disturbances in local blood perfusion, blood–brain barrier permeability or mechanical injuries to the cortical surface and bleedings.[20] In addition, the method is technically limited to retrieve information from a small field of view and to a depth of $\leq$500 μm, and is thus not capable to spatially resolve the neutrophil response in the entire brain.

Recent advances in instrumentation and image reconstruction have led to the emergence of near-infrared fluorescence (NIRF) imaging as a technique that can visualize pathological processes in intact animals using dedicated fluorescent probes and reporter technology.[21] NIRF imaging uses light in the spectral range of 700–900 nm, in which absorption of endogenous absorbers like oxy- and deoxygenated haemoglobin and water is lowest and photons can penetrate deeply into living tissue. The technique has been shown to detect fluorochromes in the brain of mice with high sensitivity.[22,23] NIRF imaging constitutes an attractive tool for investigating mouse models of cerebral ischaemia. The non-invasiveness of the technique allows to study cellular processes in the live animal with all regulatory processes preserved, without impeding animal physiology and welfare, thereby enabling repetitive assessment of the same animal. NIRF imaging has already been applied to visualize a variety of disease-relevant processes.[24–29]

Here we present an approach using adoptive transfer of fluorescently labelled neutrophils to monitor the dynamics of neutrophil accumulation in the mouse brain after the tMCAO with planar NIRF imaging. Our data revealed accumulation of neutrophils in the ischaemic brain but also in extracranial tissue. Moreover, we employed NIRF imaging to assess the role of α4-integrins in mediating neutrophil accumulation to the ischaemic brain in vivo.

Materials and methods

Animals and treatment

All procedures conformed to the national guidelines of the Swiss Federal act on animal protection and were approved by the Cantonal Veterinary Office Zurich (Permit Number: 18-2014 and 49-2011). We confirm compliance with the ARRIVE guidelines on reporting animal experiments.

Male C57BL/6J mice (Janvier, France), weighing 20–25 g, of 8–10 weeks of age were used, randomly assigned to the experimental groups. Animals were housed in a temperature controlled room in individually ventilated cages, containing up to five animals per cage, under a 12-h dark/light cycle. Paper tissue was given as environmental enrichment. Food (3437PXL15, CARGILL) and water were provided ad libitum.

Experimental protocols

VLA-4-mediated adhesion of neutrophils was blocked by intravenous infusion of rat anti-mouse α4-integrin (clone PS/2, 100 μg/mouse) 15 min prior to surgery, while control mice received rat anti-mouse endoglin (clone MJ7/18, 100 μg/mouse). Both antibodies were generated endotoxin-free in house. No randomization was applied. Using G*Power 3.1 software (Heinrich-Heine-Universität, Düsseldorf, Germany; http://www.gpower.hhu.de/), a sample size of $n \geq 10$ per group was calculated a priori for the primary end point normalized fluorescence intensities over the ipsilateral

brain at 18 h after reperfusion, assuming an effect size $d = 1.7$, at $\alpha = 0.05$ and $\beta = 0.2$. A total of 26 mice received intravenously either rat anti-α4-integrin antibody ($n = 13$) or isotype control ($n = 13$).

Focal cerebral ischaemia

Transient MCAO was induced using the intraluminal filament technique.[30] Anaesthesia was initiated by using 3% isoflurane (Abbott, Cham, Switzerland). Anaesthesia was maintained with 1.5–2% isoflurane in a mixture of O_2 (200 ml/min) and air (800 ml/min), supplied via face mask. Before the surgical procedure, a local analgesic (Lidocaine, 0.5%, 7 mg/kg) was administered subcutaneously. Temperature was controlled during the surgery and kept constant at 37 ± 0.5°C with a feedback-heating controlled pad system. For tMCAO, a midline neck incision was made and the left common carotid artery (CCA) was ligated proximal of the bifurcation of the internal carotid artery (ICA) and external carotid artery (ECA). Subsequently, the left ECA was isolated and ligated and a suture was placed around the ICA to temporarily restrict blood flow. A small incision was made in the CCA and an 11-mm long silicone-coated monofilament (171956PK5Re, Doccol Corporation, USA) was introduced and advanced until it occluded the middle cerebral artery (MCA). A suture around the ICA secured the filament in position. After occlusion of the vessel, animals were transferred to a heated recovery box and allowed to wake up. After 60 min, animals were reanaesthetized. The filament was withdrawn and the ICA was ligated. Sham-operation involved surgical procedures, without occlusion of the middle cerebral artery. After surgery buprenorphine was administered as s.c. injection (Temgesic, 0.1 mg/kg b.w.) and animals were placed in a heated recovery box for 2 h. Buprenorphine was then given twice s.c. every 6–8 h on the day of surgery and thereafter supplied via drinking water (1 mg/kg) for 36 h. Animals receive softened chow in a Petri-dish placed on the floor of their cages to encourage eating. Animals were excluded from the studies when they fulfilled one of the following criteria: prolonged surgery time (>15 min); no reflow after filament withdrawal; dead before experimental endpoint. Mortality rate was 0%.

Characterization of the neutrophil response in the blood

Whole blood (≥50 µl) was collected by saphena vein punctuation into EDTA-coated tubes (Sarstedt, Nümbrecht, Germany) 3 times prior to tMCAO (baseline), at 0.5, 1.5, 4, 24 or 48 h after reperfusion or corresponding sham surgery in a random fashion ($n \geq 9$ per time point). Samples were incubated at room temperature (RT) for 15 min with both an anti-Ly6G-PE (clone 1A8) and an anti-Ly6G/Ly6C-APC antibody (clone Gr1, both BD Pharmingen, Germany), followed by a red blood cell lysis containing 1.5% PFA (500 µl, 10 min, RT, BD Pharmingen, Switzerland) and kept on ice until they were analysed with a Gallios™ Flow Cytometer (Beckman Coulter, Switzerland). Up to 10,000 events were acquired and examined for the expression of Ly6C and Ly6G using the Kaluza Analysis Software (Beckman Coulter, USA).

Isolation of neutrophils from bone marrow

Mice were sacrificed by cervical dislocation after given deep 3% isoflurane anaesthesia. Femur and tibia from both legs were removed, and the extreme distal tip of each bone was cut off under sterile conditions and bone marrow was flashed out with HBSS. After dispersing cell aggregations, red blood cells were lysed with 20 ml of a 0.83% ammonium chloride and Tris-HCl 9:1 (pH 7.5) buffer. Lysis was stopped by adding 30 ml HBSS. The suspension was centrifuged (400 g, 6 min, 4°C) and cell pellet was resuspended in 10 ml HBSS. Neutrophils were separated through two Percoll gradient (GE Healthcare, Uppsala, Sweden) centrifugations steps (64.8% and 61.5% Percoll, 1000 g, 20 and 35 min, 4°C). We obtained $5 \pm 1.5 \times 10^6$ neutrophils per mouse.

Fluorescent labelling of neutrophils and viability assay

To identify a suitable NIRF dye for neutrophil labelling neutrophils were incubated in HBSS (0.2×10^6 cells/10 µl) for 15 min at RT together with either 5, 10, 25 or 50 µg/ml of VivoTrack680 (Perkin Elmer, USA) or LIPO-6S-IDCC (Freie Universität Berlin, Germany). To establish the optimal LIPO-6S-IDCC concentration, neutrophils were incubated with either 5, 10, 25, 50, 100, 250 or 500 µg/ml of dye for 15 min. To determine the optimal incubation time, neutrophils were incubated with 25 µg/ml of LIPO-6S-IDCC for 5, 10, 15, 20, 25 or 30 min. Fluorescence was measured using a Gallios™ Flow Cytometer. To assess cell viability, 10 µl of an aqueous solution of propidium iodide (0.1 mg/ml) was added 10 s before flow cytometric analysis. Electronic gating was used to differentiate viable cells from apoptotic cells.

Neutrophil activation assays

LIPO-6 S-IDCC labelled or unlabelled neutrophils isolated from two animals were resuspended in Dulbecco's phosphate-buffered saline supplemented with 2.5% calf serum and 0.1% NaN_3. Aliquots of 0.3×10^6 neutrophils per 200 µl were distributed in a 96-well round bottom microtiter plate and centrifuged at 330 g at

4°C for 3 min. The pellets were dislodged and incubated with the following directly conjugated rat antibodies at 10 µg/ml for 30 min on ice: CD45 APC (BioLegend 103112, clone 30F11); Ly6G APC/Cy7 (BioLegend127624, clone 1A8); LFA-1 FITC (CD11a, BD 01204D, clone 2D7); Mac-1 PB (CD11b, BioLegend 101224, clone M1/70); CD49d PE (integrin-α4, Southern Biotech 1520-09, clone PS/2); PSGL-1 AF647 (clone 4RA10, conjugated in house); L-selectin FITC (CD62L, BD 553150, clone Mel-14). In parallel, selected aliquots were incubated with appropriate isotype controls. Last, all cells were washed several times and fixed with 1% PFA/PBS for flow cytometry.

NIRF imaging

NIRF imaging was performed with the Maestro 500 multispectral imaging system (Cambridge Research & Instruments Inc, USA). A band pass filter (615–665 nm) was used for excitation. The fluorescence was detected by a CCD camera fitted with a long pass filter (700 nm). Fluorescence emission images were acquired by incrementally increasing the excitation wavelengths over the indicated range. NIRF images were subjected to spectral unmixing using the CRi Maestro Image software.

Determination of detection sensitivity in a silicone phantom

A tissue like silicone phantom was produced as previously described.[31] The absorption coefficient (μ_a) of 0.2 cm^{-1} and a scattering coefficient (μ'_s) of 10 cm^{-1} were adapted to match the optical properties of the brain. Exchangeable micropipettes (volume 1 µl per 15 mm, Brand GmbH & Co. KG, Germany) were placed in a hole at 2 mm depth parallel to the surface of the phantom (Figure 3(b)). Micropipettes containing either 750, 1000, 1750, 2500, 5000 or 10,000 neutrophils/µl were placed within the phantom for NIRF imaging. Image analysis consisted of drawing a region of interest (ROI) over the area containing the neutrophil suspension, measuring the average fluorescence intensity of all pixels within the ROI divided by the factor of their area.

NIRF imaging in vivo

LIPO-6S-IDCC-labelled neutrophils ($7.5 \times 10^6 \pm 0.5 \times 10^6$ cells) were adoptively transferred by intravenous injection 15 min prior to tMCAO or sham surgery. To establish the time course of neutrophil accumulation, 31 mice were serially imaged in a staggered design up to 6 times within 48 h (sham n = 9–15 and tMCAO n = 7–10). For the anti-α4-integrin treatment study mice were serially imaged at 18 h (isotype control n = 11; rat anti-α4-integrin n = 10), 24 h (isotype control n = 12; rat anti-α4-integrin n = 11) and 48 h after tMCAO (isotype control n = 12; rat anti-α4-integrin n = 12). In few animals, we missed the time point for imaging. Mice were anaesthetized with 1.5–2% isoflurane in an oxygen/air mixture (1:4) and the skin overlying the head was depilated. Animals were placed onto an animal support into which a warm-water circuit was integrated to maintain body temperature. ROIs were manually drawn over the right and left hemisphere and temporal muscles (Figure 4(a)). The person was blinded to the experimental group. Animals with skin irritations or wounds were excluded from analysis. The average fluorescence intensity of all pixels within the ROI were measured and divided by the factor of their area. Normalized fluorescence intensities were calculated by dividing the mean fluorescence intensity of the ipsilateral side by the mean fluorescence intensities of the contralateral side X 100.

Tissue processing

Animals were put under deep anaesthesia by intraperitoneal injection of ketamine/xylazine/acepromazine maleate (100/20/3 mg/kg body weight) and transcardially perfused with 20 ml PBS, followed by 1% paraformaldehyde in PBS (pH 7.4; PFA). For images shown in Figure 1 and 5 paraffin embedding of tissue was performed. Whole heads were removed and fixed in 4% PFA for approximately 48 h (mice sacrificed after 24 h of reperfusion after tMCAO) after removal of the skin. Cuts between the eyes and removing of the occipital plates were performed to ensure PFA access to the brain. Skulls were decalcified in Citrate EDTA Buffer pH 7.5 (Quartett, Germany) for 7 days, then sliced (coronary sections, 2-mm slices, caudal direction from nose) and routinely paraffin wax embedded.

For images shown in Figure 4, brains were immediately removed and sliced (coronary sections at Bregma -1 ± 0.3 mm and -5.1 ± 0.1 mm), snap frozen in Tissue-TEK® O.C.T. (Sysmex Suissie AG, Switzerland) in a 2-methylbutane (Sigma-Aldrich, Switzerland) dry ice bath and stored at −80°C.

Histology and immunohistochemistry

Consecutive 5-µm-thick sections were prepared from frozen brain blocks and paraffin blocks from the heads (coronary sections) and were either stained with haematoxylin and eosin (HE, Sigma-Aldrich) or subjected to immunohistochemistry for the demonstration of neutrophils as described before.[32] Cryosections were fixed with acetone for 10 min at −20°C and rehydrated

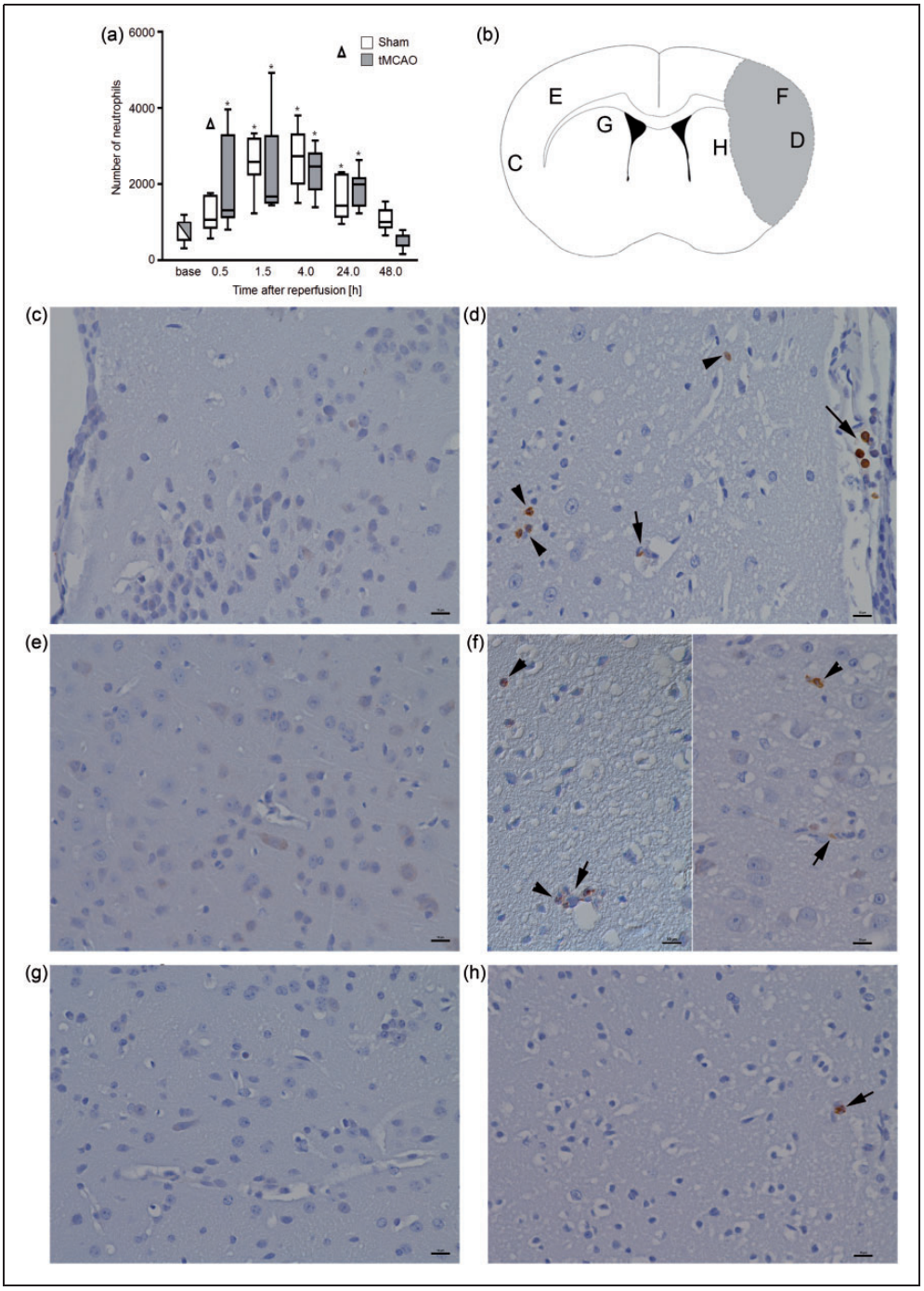

Figure 1. Systemic neutrophil mobilization and attraction to the site of ischaemic damage following tMCAO. (a) Flow cytometry showed a significant increase in the amount of circulating neutrophils at 1.5 and 4 h of reperfusion after 1 h of tMCAO (grey) or sham surgery (white), but dropped to pre-surgery levels thereafter. Neutrophil levels in sham and tMCAO animals did not differ significantly. These results are indicative of neutrophil mobilization as an immediate response to surgery. Centre lines show the medians; box limits indicate the 25th and 75th percentiles; whiskers extend 1.5 times the interquartile range from the 25th and 75th percentiles. Repeated-measures ANOVA and Holm–Sidak, baseline n = 13, sham n = 9, MCAO n = 9–11 per group for all time points, *$p < 0.05$ vs baseline. (b) Sketch to highlight the location and extent of the ischaemic lesion in a coronal brain section (Bregma 0.74 mm), and indicating where images (c–h) were acquired. (c–h) Representative images of a mouse brain after 1 h of tMCAO and 24 h after reperfusion to show the presence and distribution of neutrophils (Ly6G+) in paraffin sections. (c,e,g) Contralateral hemisphere showing no neutrophil influx in the leptomeninges (c), cortex (c,e) and striatum (g). (d,f,h) Inspection of the ipsilateral hemisphere revealed that Neutrophils are present in low numbers within leptomeningeal vessels (d, long arrow) and individually within parenchymal vessels (short arrows) in cortex (d,f) and striatum (h). A few individual neutrophils are also seen outside blood vessels, in the parenchyma (arrowheads). Avidin biotin complex method, haematoxylin counterstain. Bars = 10 μm.

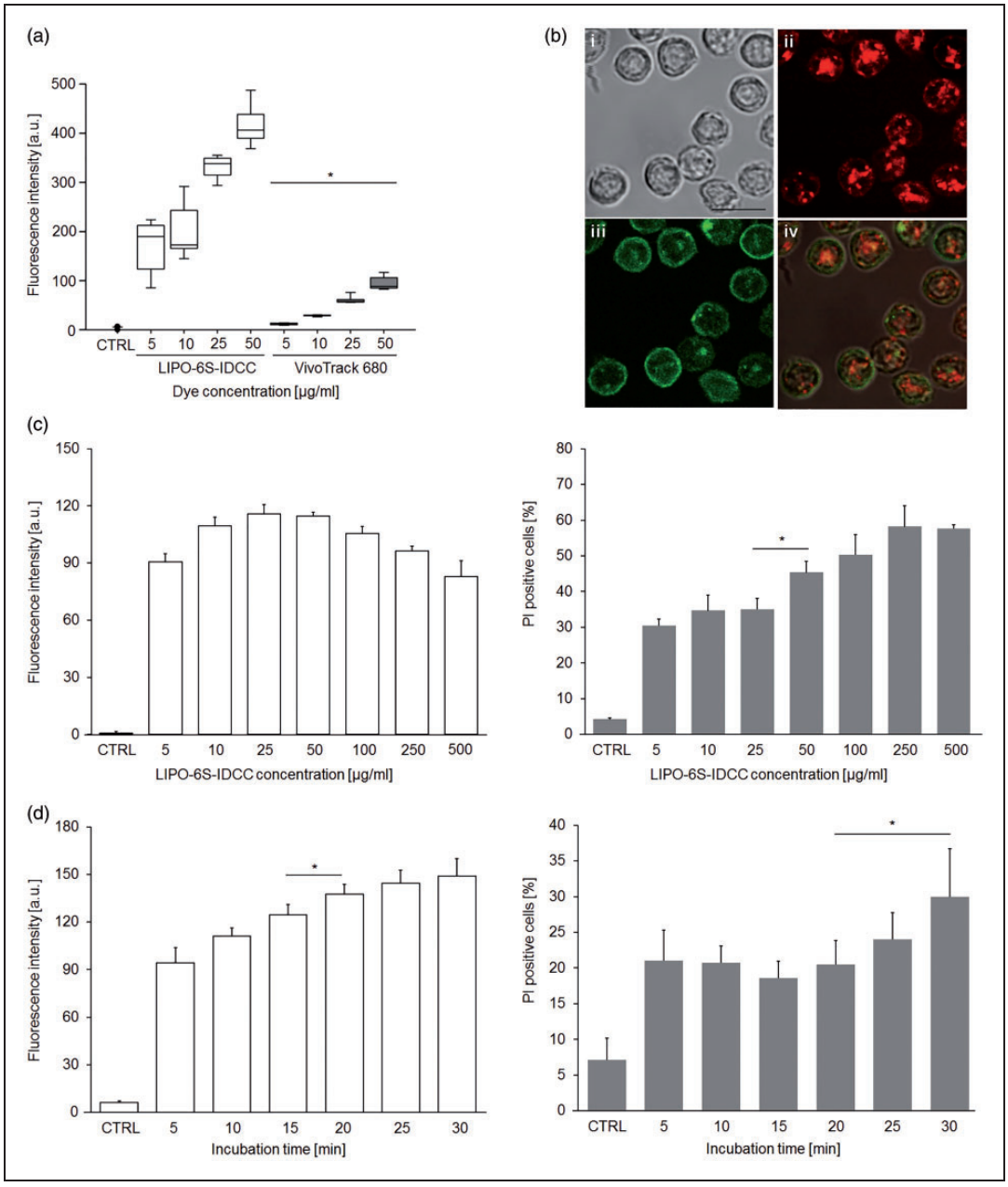

Figure 2. Labelling of neutrophils for NIRF imaging. (a) Comparison of the fluorescence intensities measured by flow cytometry after incubation of neutrophils with different concentrations of LIPO-6S-IDCC and VivoTrack 680. Centre lines show the medians; box limits indicate the 25th and 75th percentiles; whiskers extend 1.5 times the interquartile range from the 25th and 75th percentiles. $n = 9$; *$p < 0.05$ by repeated-measures ANOVA and Tukey's test. (b) Confocal microscopy images of neutrophils after incubation with LIPO-6S-IDCC and anti-Ly6G-PE antibody. Depicted are cells in the (i) transmitted light, (ii) LIPO-6S-IDCC red channel, (iii) Ly6G green channel and (iv) the overlay. Bar = 10 µm. (c) Incubation of neutrophils with different concentrations of LIPO-6S-IDCC. The propidium iodide assay was used to assess the effect of labelling on cell viability. Mean ± SD; $n = 3$ animals with three independent experiments each, *$p < 0.05$ by one-way ANOVA with Tukey's posttest. (d) Incubation of neutrophils with 25 µg/ml LIPO-6S-IDCC for different time intervals. Mean ± SD, $n = 3$ animals with three independent experiments each; *$p < 0.05$ by one-way ANOVA with Tukey's posttest. CTRL = control.

in PBS for 5 min. Sections prepared from paraffin embedded heads were deparaffinized and incubated with citrate buffer (pH 6.0, 20 min at 98°C) for antigen retrieval. Incubation with the primary rat anti-Ly6G antibody (clone 1A8, Biolegend) was performed for deparaffinized sections at 4°C for 15–18 h and for cry-sections at RT for 1 h, respectively. All sections were subsequently incubated with a biotinylated secondary

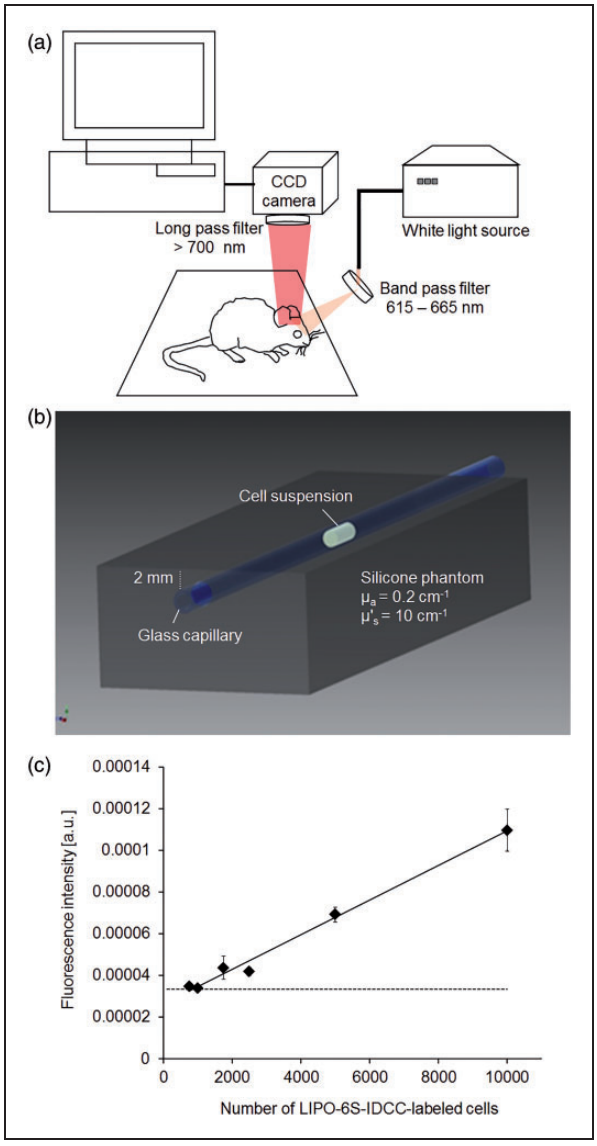

Figure 3. Fluorescence intensity as a function of the number of labelled neutrophils. (a) Set-up for NIRF imaging. Excitation light from a white light source is filtered and directed to the mouse head. Fluorescence is detected using a charged-couple device (CCD) camera fitted with adequate emission filters. (b) Illustration of a silicon phantom mimicking brain tissue. A glass capillary was inserted at a depth of 2 mm and filled with suspensions containing different numbers of LIPO-6S-IDCC-labelled neutrophils. (c) Fluorescence intensities as a function of the number of LIPO-6S-IDCC-labelled neutrophils. Fluorescence intensities were measured in a region of interest of 15 mm × 6 mm over the centre of the phantom. Mean ± SD of three independent experiments.

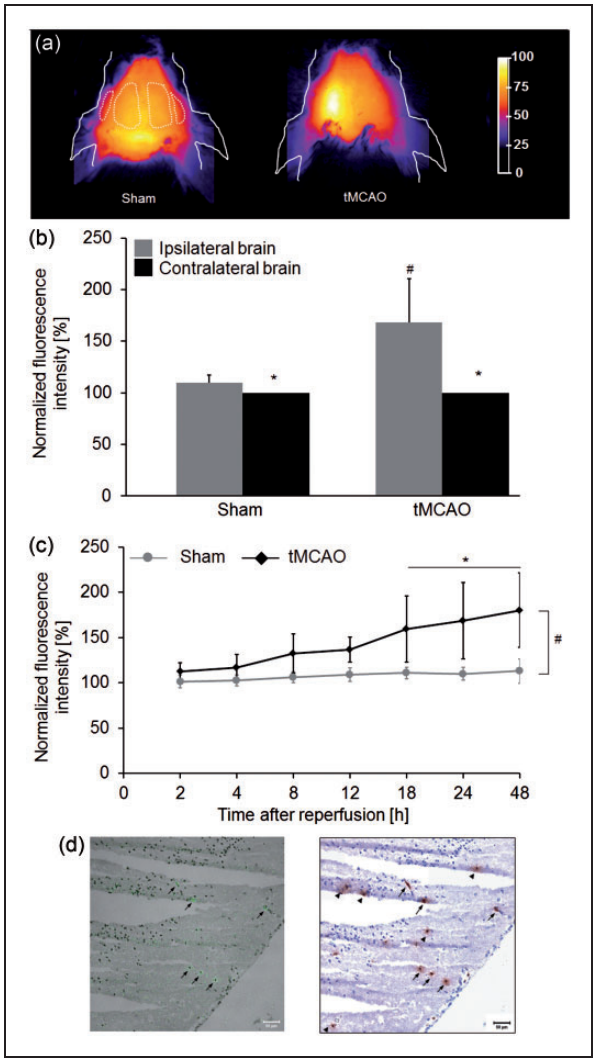

Figure 4. Tracking of neutrophils to the ischaemic lesion in C57BL/6 mice in vivo. (a) In vivo NIRF images of the mouse head. Depicted are a sham-operated mouse 25 h after adoptive transfer of LIPO-6S-IDCC-labelled neutrophils (left) and a mouse subjected to 1 h tMCAO and 24 h of reperfusion in which LIPO-6S-IDCC-labelled neutrophils were adoptively transferred prior to ischaemia (right). Examples of regions of interests drawn over the brain hemispheres and muscle regions are shown (dashed line). (b) Normalized fluorescence intensities over the ipsilateral ischaemic and contralateral brain regions. Mean ± SD; sham n = 15, tMCAO n = 10; Kruskal–Wallis one-way ANOVA followed Dunn's pairwise multiple comparison; *$p < 0.05$ vs contralateral, $^{\#}p < 0.05$ vs sham. (c) The time course of neutrophil accumulation in the brain was assessed with non-invasive NIRF imaging. Mean ± SD, sham n = 9–15, tMCAO n = 7–10 per group for all time points; repeated-measures ANOVA and Holm–Sidak pairwise multiple comparison; *$p < 0.05$ vs 2 h, $^{\#}p < 0.05$ vs sham (d) Fluorescence microscopy of cryosections of a tMCAO mouse brain 18 h after injection of labelled neutrophils. Avidin biotin complex method, haematoxylin counterstain. Shown are LIPO-6S-IDCC-labelled neutrophils (arrows) and endogenous ($Ly6G^{+}$) neutrophils (arrow head). Bars = 50 μm.

anti-rat antibody (RT, 30 min) and thereafter with a preformed streptavidin–biotin complex (RT, 30 min; both Vectastain ABC-Kit, Vector Laboratories, USA). Visualization with diaminobenzidin or

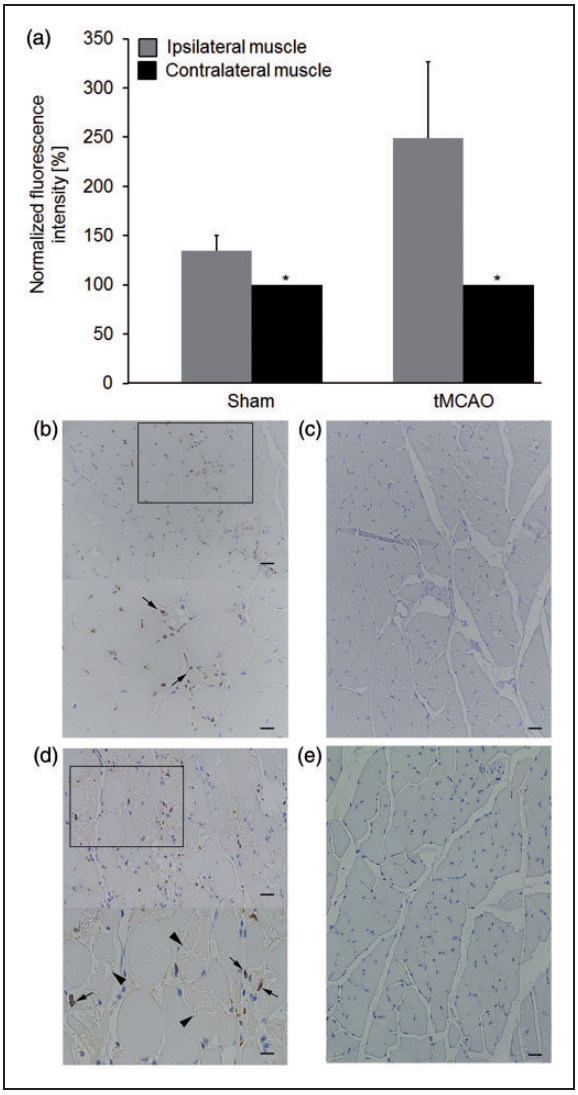

Figure 5. Neutrophil accumulation in the temporal muscle after external carotid artery ligation. (a) Fluorescence intensities measured over the left (ipsilateral) and right (contralateral) temporal muscles of sham-operated mice and animals subjected to 1 h of tMCAO and 24 h of reperfusion. LIPO-6S-IDCC-labelled neutrophils were intravenously injected 15 min prior surgery and NIRF imaging was performed 24 h after the intervention. Mean ± SD, sham n = 15 and tMCAO n = 10; Kruskal–Wallis one-way ANOVA followed Dunn's pairwise multiple comparison; *$p < 0.05$ vs contralateral. (b–e) Ly6G immunohistochemistry with avidin biotin complex method and haematoxylin counterstain of paraffin sections of the temporal muscle. (b) Ipsilateral and (c) contralateral temporal muscle of a sham-operated mouse. (d) Ipsilateral and (e) contralateral temporal muscle of a mouse subjected to tMCAO. (b,d) Individual neutrophils were observed within interstitial vessels (arrows in high magnification insets) in the ipsilateral muscles of both sham-operated and tMCAO mice. In the muscle of the tMCAO mouse, individual degenerate myofibres are observed (arrow heads in high magnification inset). (c,e) The contralateral temporal muscles were unaltered. Bar = 20 μm (overviews) and 10 μm (high magnification insets).

peroxidase substrate (AEC Kit, Vector Laboratories) was followed by haematoxylin (Sigma-Aldrich) counterstaining. All sections were mounted with an aqueous medium (Aquatex, Millipore). To assess the effects of α4-integrin blockade on neutrophil numbers, brain sections were inspected by a person blinded to the treatment group.

Detection of LIPO-6S-IDCC labelled neutrophils in brain sections

To differentiate adoptively transferred LIPO-6S-IDCC positive from endogenous neutrophils, cryosections (7 μm) were subjected to a Ly6G immunohistochemistry (described above) and imaged with a LSM710 (Zeiss, Germany) for fluorescence and a Panoramic Digital Slide Scanner (3DHISTEC, Hungary) to obtain brightfield images. Images were co-registered after imaging.

Neutrophil count

Absolute numbers of $Ly6G^+$ neutrophils were determined at five levels spanning the entire lesion, i.e. at Bregma +2.8, +1.54, +0.14, −1.94 and −4.6 mm, in both hemispheres. We differentiated between neutrophils located to the meninges and parenchymal cells. The latter term was used for simplification only and does not imply extravasation of neutrophils into the brain parenchyma.

Determination of cerebral lesion volumes

Five 7 μm thick coronal HE-stained cryosections (taken at Bregma +2.8, +1.54, +0.14, −1.94 and −4.6 mm) were digitized with a Panoramic Digital Slide Scanner (3DHISTEC, Hungary) at 20× magnification. Lesions were determined with NDP.view.4.26 (Hamamatsu Photonics K.K.). The person was blinded with respect to the treatment groups. Cerebral lesion volumes were calculated by summing up the volumes of each section and correcting for oedema (isotype control group n = 10; anti-α4-integrin treated n = 13).

Statistical analysis

Data are presented as mean ± SD. Comparisons were made by one-way ANOVA or repeated measures ANOVA followed by Holm–Sidak or Tukey's test, ANOVA on ranks followed by Dunn's test, or Mann–Whitney rank sum test where applicable. A Spearman's correlation analysis was performed between the number of neutrophils in the phantom and measured fluorescence intensities. A p-value < 0.05 was considered significant.

Results

Systemic neutrophil mobilization and neutrophil attraction to the ischaemic territory after tMCAO

To evaluate effects of the placement of the intraluminal filament on the number of circulating neutrophils, we serially quantified blood neutrophils after 1 h of tMCAO in male C57BL/6 mice using flow cytometry (the gating strategy is shown in Supplementary Figure 1). Serial blood samples were taken from C57BL/6 mice, prior to and 0.5, 1.5, 4, 24 and 48 h after 1 h of tMCAO or sham-surgery (Figure 1(a)). Neutrophil counts were significantly higher in the blood of sham mice at 1.5, 4 and 24 h, while in tMCAO mice significant higher neutrophil counts were detected at 0.5, 1.5, 4 and 24 h after reperfusion ($p < 0.05$ vs baseline). There were no statistical significant differences between sham and tMCAO animals at 0.5, 1.5, 4 and 24 h after reperfusion ($p > 0.05$ pairwise comparison). This indicates that the systemic neutrophil response was dominated by the surgical intervention required in this model.

We next analysed the ischaemic brain lesion in tMCAO mice for the presence of neutrophils at 24 h after reperfusion (Figure 1(c–h)), as it has previously been shown that neutrophils are most abundant in the brain between 18 and 24 h after tMCAO.[32] As expected,[33] the lesion induced by 1 h of tMCAO and 24 h of subsequent reperfusion was represented by extensive necrosis and oedema in the striatum and neocortex that extended beyond the middle cerebral artery territory within the ipsilateral hippocampus and thalamus. Neutrophils ($Ly6G^+$) were found in association with the lesions in low numbers. They were predominantly seen individually within small vessels in the adjacent leptomeninges and the affected parenchyma, occasionally also outside vessels in the affected parenchyma (Figure 1(d,f,h)), confirming previous reports.[32,34] The contralateral hemisphere was generally free from neutrophils (Figure 1(c,e,g)). In brains of sham-operated mice, only few $Ly6G^+$ cells were detected in leptomeningeal vessels (data not shown). This confirms that neutrophils are recruited into the brain as a consequence of the ischaemic tissue injury.

Plasma membrane labelling of neutrophils for NIRF imaging does not lead to cell activation

NIRF imaging requires labelling of neutrophils, a procedure which should ideally neither alter the phenotype nor the function of neutrophils. We aimed at establishing a protocol for ex vivo labelling of neutrophils isolated from the bone marrow of C57BL/6 mice. Purified neutrophils were incubated with the NIRF dyes VivoTrack680 or LIPO-6S-IDCC at different dye concentrations. Cells showed higher fluorescence intensities when labelled with LIPO-6S-IDCC compared with VivoTrack680 at all concentrations tested (Figure 2(a), LIPO-6S-IDCC 173 ± 52, 198 ± 54, 332 ± 21, 414 ± 37 vs VivoTrack680 12 ± 2, 29 ± 1, 60 ± 6, 94 ± 12, $p < 0.05$). Confocal microscopy revealed that LIPO-6S-IDCC labels the plasma membranes of $Ly6G^+$ cells (Figure 2(b)). To determine the optimal dye concentration for neutrophil labelling, we incubated equal numbers of harvested neutrophils with different amounts of LIPO-6S-IDCC dye for 15 min and analysed the samples by flow cytometry (Figure 2(c)). In addition, neutrophils were incubated with propidium iodide to assess adverse effects on cell viability. Fluorescence emission increased with increasing concentrations of LIPO-6S-IDCC with a maximum at 25 μg/ml LIPO-6S-IDCC. Thereafter, fluorescence intensities decreased, likely due to self-quenching. The proportion of non-viable neutrophils was higher in LIPO-6S-IDCC than in unlabelled cells at all concentrations tested (Figure 2(c)), and concentrations above 50 μg/ml led to a further increase in the number of non-viable cells. Furthermore, to find the optimal incubation time, we incubated neutrophils with 25 μg/ml of LIPO-6S-IDCC for different periods of time (Figure 2(d)). Flow cytometry revealed increasing fluorescence emission with increasing incubation times, but with incubation times longer than 20 min, the proportion of non-viable cells increased significantly. Thus, a concentration of 25 μg/ml LIPO-6S-IDCC and an incubation time of 20 min constituted a good compromise between cell viability and fluorescence intensity.

To determine whether in vitro labelling of neutrophils with LIPO-6S-IDCC results in their activation, neutrophils were isolated from the bone marrow of two C57BL/6 mice and pooled. Half of the cells were incubated with 25 μg/ml LIPO-6S-IDCC for 20 min, while the unlabelled fraction served as control. Cells were stained with directly conjugated rat antibodies recognizing CD45, Ly6G, CD62L (L-selectin), CD11a (LFA-1) and CD11b (Mac-1). Cell surface expression of the activation markers CD62L, CD11a and CD11b on $Ly6G^+/CD45^+$ neutrophils was assessed by flow cytometry (Supplementary Figure 2A). LIPO-6S-IDCC labelling induced only negligible shedding (reduction of 8%) of membrane associated L-selectin (CD62L) compared with unlabelled cells (Supplementary Figure 2B). In addition, we did not detect an increased expression of CD11a and CD11b on neutrophils in response to the labelling procedure with LIPO-6S-IDCC (Supplementary Figure 2C, D), underscoring that this labelling procedure does not activate the neutrophils.

NIRF imaging enables monitoring of neutrophil accumulation to the ischaemic lesion in vivo

For the non-invasive whole brain visualization of neutrophil trafficking, we have used a planar NIRF imaging system operated in reflectance mode (Figure 3(a)). Light from a white light source was directed through a band pass filter to the head of the anaesthetized animal. The emitted fluorescence was captured using a CCD camera fitted with adequate emission filters and a lens to adjust the focal plane. To evaluate the capacity of NIRF imaging to detect fluorescently labelled neutrophils, we first used brain tissue mimicking silicon phantoms (Figure 3(b)). To simulate optical tissue properties of the mouse brain, TiO_2 particles and carbon black powder were added as scattering and absorbing agent, respectively. Different numbers of LIPO-6S-IDCC-labelled neutrophils in suspension were filled into a glass capillary, which was inserted at a 2 mm depth below the surface of the phantom. We found a linear correlation between the measured fluorescence intensities and the number of neutrophils in the centre of the glass capillary (Figure 3(c), $R^2 = 0.98$, $p < 0.05$). A minimum number of 1750 LIPO-6S-IDCC-labelled neutrophils in a volume of 1.5 µl could be distinguished from the background of the phantom.

For NIRF imaging of neutrophil accumulation in the ischaemic brain in vivo, we intravenously injected $7.5 \pm 0.5 \times 10^6$ LIPO-6S-IDCC-labelled neutrophils into mice 15 min prior to tMCAO. NIRF imaging was performed 24 h after reperfusion (Figure 4(a,b)). Sham-operated animals injected with LIPO-6S-IDCC-labelled neutrophils served as controls. In tMCAO mice and sham-operated animals, injection of fluorescently labelled neutrophils resulted in significant higher fluorescence intensities over the left ischaemic hemisphere compared with the contralateral hemisphere (ipsilateral tMCAO $168 \pm 42\%$, ipsilateral sham $111 \pm 4\%$ vs contralateral, $p < 0.05$). Yet, the fluorescence intensities were significantly higher in tMCAO animals as compared with shams ($p < 0.05$). To establish the time course of neutrophil trafficking to the brain in vivo, we adoptively transferred LIPO-6S-IDCC-labelled neutrophils before tMCAO and recorded fluorescence intensities longitudinally with NIRF imaging (Figure 4(c)). We observed a steady increase in fluorescence over the ischaemic hemisphere in tMCAO mice injected with LIPO-6S-IDCC-labelled neutrophils. Normalized fluorescence intensities were significantly higher in the interval at 18 to 48 h compared with 2 h after reperfusion ($p < 0.05$). In sham-operated mice, there was only a minor increase in normalized fluorescence intensities observed over the ipsilateral hemisphere. Normalized fluorescence intensities in the ipsilateral hemisphere was significantly higher in tMCAO at all time points ($p < 0.05$). A subgroup of tMCAO animals that were injected with LIPO-6S-IDCC-labelled neutrophils were sacrificed at 18 h after reperfusion. Fluorescence microscopy and immunohistochemistry demonstrated that both exogenously labelled neutrophils and endogenous neutrophils ($Ly6G^+$) were present in the ischaemic territory (Figure 4(d)). The LIPO-6S-IDCC-labelled neutrophils made up approximately 50% of all neutrophils and appeared morphologically unaltered. Taken together, these finding indicates that labelled neutrophils are recruited to the site of ischaemic injury.

Interestingly, we detected significantly higher normalized fluorescence intensities over the ipsilateral temporal muscle compared with the contralateral side in tMCAO mice and sham-operated mice at 24 h of reperfusion (Figure 5(a), ipsilateral tMCAO $249 \pm 76\%$, ipsilateral sham $135 \pm 16\%$ vs contralateral, $p < 0.05$). There was no significant difference in normalized fluorescence intensities of the ipsilateral muscle between sham and tMCAO animals ($p > 0.05$). This prompted us to further investigate the source of the fluorescence signal. Ly6G immunohistochemistry identified presence of numerous neutrophils in the ipsilateral muscle mainly in interstitial vessels in sham and tMCAO animals, which was not observed in the corresponding contralateral temporal muscles (Figure 5(b–e)). These findings indicate that the fluorescence signal originated not from the ischaemic lesion but is due to neutrophil trafficking into the temporal muscle.

α4-integrins mediate post-ischaemic neutrophil accumulation in the CNS in vivo

Intravascular guiding cues direct neutrophils to sites of tissue damage.[4] In light of a recent study proposing binding of neutrophils via VLA-4,[19] we investigated the effect of a blockade of α4-integrins on neutrophil trafficking with NIRF imaging. The α4-integrin subunit can pair with the β1-integrin subunit to form VLA-4, which binds to VCAM-1,[35] fibronectin and JAM-B on brain endothelial cells in the mouse. Blockade of α4-integrin by the monoclonal antibody PS/2 significantly reduced the interaction of neutrophils with cerebral blood vessels at the site of ischaemic cerebral injury and consecutively reduced the damage in the tMCAO model.[19] We serially performed NIRF imaging at 18, 24 and 48 h of reperfusion following antibody-mediated inhibition of α4-integrins. In each group, one mouse had to be excluded from analysis due to skin irritation caused by epilation procedure. Anti-α4-integrin antibody treated animals had significantly reduced fluorescence intensities over the left ischaemic hemisphere at 18 and 24 h after tMCAO compared with animals that received a control antibody (Figure 6(a),

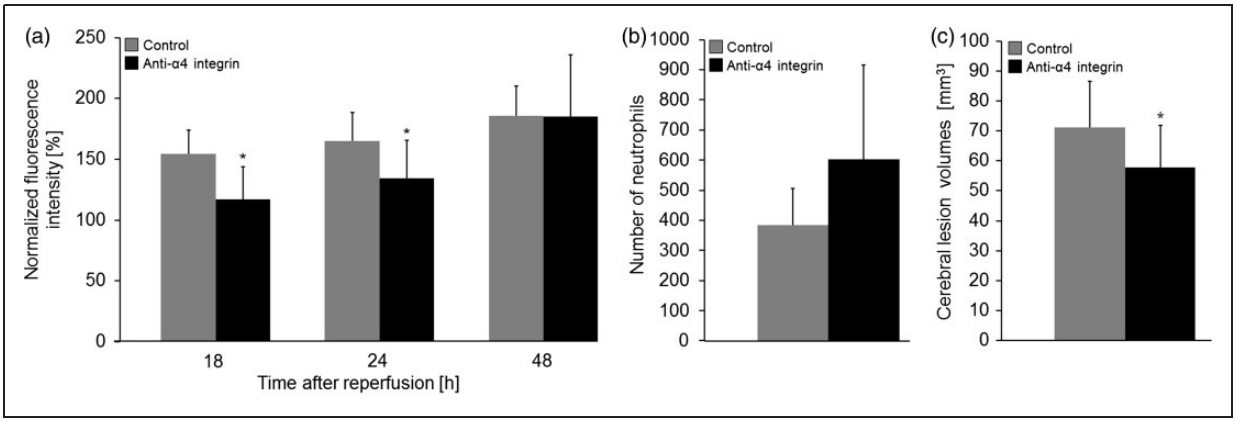

Figure 6. α4-integrins mediate neutrophil accumulation to the ischaemic lesion in vivo. (a) Normalized fluorescence intensities measured over the ischaemic hemisphere of mice. Mean ± SD, anti-α4-integrin n = 10–12, control n = 11–12, Mann–Whitney rank sum test, *$p < 0.05$. (b) Absolute numbers of Ly6G$^+$ neutrophils were determined in anti-Ly6G stained brain cryosections at five levels spanning the entire lesion, i.e. at Bregma +2.8, +1.54, +0.14, −1.94 and −4.6 mm, in both hemispheres. Mean ± SD, anti-α4-integrin, n = 4, control n = 5, Mann–Whitney rank sum test, *$p < 0.05$. (c) Oedema corrected cerebral lesion volumes at 48 h after reperfusion. Mean ± SD, anti-α4-integrin n = 13, control antibody, n = 10, Mann–Whitney rank sum, *$p = 0.05$ vs control antibody.

anti-α4-integrin 117 ± 27% and 135 ± 31% vs control antibody 155 ± 19% and 165 ± 23%, $p < 0.05$), indicating substantially reduced neutrophil accumulation in the ischaemic hemisphere. At 48 h, fluorescence intensities were not significantly different between anti-α4-integrin antibody treated animals and controls (anti-α4-integrin antibody 185 ± 51% vs control antibody 186 ± 25%, $p > 0.05$). For cross-validation, we counted neutrophils in brain sections of a subgroup of animals euthanized at the endpoint at 48 h after reperfusion (Figure 6(b)). We found no significant differences in the total number of neutrophils between the two groups (anti-α4-integrin antibody 603 ± 313 vs control antibody 384 ± 123, $p > 0.05$). Moreover, we assessed the effect of anti-α4-integrin antibody on the ischaemic damage on HE stained tissue cryosections (Figure 6(c)). Three brains of the control group were excluded due to damage during tissue processing. Cerebral lesion volumes were reduced by 19% in anti-α4-integrin antibody treated as compared with control antibody treated animals 48 h after reperfusion (anti-α4-integrin antibody 57.8 ± 14.0 mm^3 vs 71.2 ± 15.3 mm^3, $p < 0.05$) concomitant with an early reduction of neutrophil accumulation.

Discussion

In the current study, we used NIRF imaging to non-invasively track fluorescently labelled and adoptively transferred neutrophils to the ischaemic brain in mice. We have isolated neutrophils from the bone marrow of C57BL/6 mice, which have been previously shown to be morphologically mature and functionally competent.[36] We first established an optimized protocol for labelling neutrophils ex vivo with the NIRF dye LIPO-6S-IDCC minimizing negative effects of the labelling on cell viability with increasing dye concentrations and incubation times. In addition, we examined whether the labelling procedure leads to neutrophil activation, which would be undesirable for trafficking studies. Most leukocytes constitutively express L-selectin mediating tethering and rolling along the endothelium. Upon activation of the leukocytes, the extracellular domain of L-selectin is generally shed from the surface.[37] In parallel, it is widely acknowledged that the surface expression of Mac-1 (CD11b/CD18, aMb2) is increased due to mobilization of intracellular reservoirs.[38] Surface levels of LFA-1 (CD11a/CD18, aLb2) do not seem to be affected in that process.[39] We observed only minute shedding of L-selectin in the LIPO-6S-IDCC labelled neutrophil population and surface expression of aMb2 and aLb2 integrins was indistinguishable between labelled and unlabelled neutrophils. This underscores that the labelling does not trigger activation of labelled neutrophils to a significant level.

Non-invasive monitoring of neutrophil recruitment puts high demand on the detection sensitivity of the imaging methods because neutrophil accumulation in the mouse brain after tMCAO was reported to be relatively low.[40,32,34] We have found that NIRF imaging can detect as few as 1750 LIPO-6S-IDCC-labelled neutrophils in a homogenous phantom mimicking brain tissue. However, when non-invasively imaging the mouse head contributions from all compartments of the head including skin, bone, muscles, meninges, and brain have to be considered. Hence, generation of a detectable contrast does not only depend on the number of accumulated cells in the ischaemic territory

but also on the optical properties of the various tissue compartments and the biodistribution of the labelled cells after adoptive transfer.

The injection of LIPO-6S-IDCC-labelled cells in sham-operated animals led to an increase in fluorescence of both hemispheres with a minor contrast between the ipsi- and contralateral side. The fluorescence of the contralateral hemisphere is likely due to labelled neutrophil circulating in the blood (5–10% of the total neutrophils) and in the bone marrow of the skull, which is a main site of neutrophil clearance.[41] The slightly higher fluorescence on the ipsilateral side is likely due to a spillover from the fluorescence of accumulated neutrophils in the temporal muscle.

Fluorescence intensities over the ipsilateral hemisphere were significantly higher in tMCAO mice that received LIPO-6S-IDCC-labelled cells than in the corresponding sham-operated animals. Using fluorescence microscopy, we found accumulation of LIPO-6S-IDCC-labelled neutrophil at the ischaemic territory, confirming that the detected NIRF contrast is due to the accumulation of adoptively transferred neutrophils.

Longitudinal NIRF imaging in ischaemic mice revealed an early presence of neutrophils starting immediately after onset of reperfusion, which shows that neutrophils are among the first immune cells that respond to an ischaemic insult. Neutrophil accumulation peaked at 18 h after reperfusion. Previous studies assessing neutrophil accumulation in the brain of C57BL/6 mice after 1 h of tMCAO using flow cytometry and immunohistochemistry showed considerably variability in dynamics, i.e. to peak at 18–24 h,[32] at 48 h[42] and at 3 days after reperfusion.[40] Fluorescence signals from neutrophils in the ischaemic hemisphere remained elevated up to 48 h after reperfusion, indicating that neutrophils might have a prolonged lifespan, compared with 11 h under homeostatic conditions,[43] which is mediated by pro-survival cytokines and chemokines in the ischaemic lesion.[44] Taken together, the findings show that NIRF imaging is capable to non-invasively monitor the dynamics of the neutrophil response after cerebral ischaemia in vivo. A general disadvantage of the presented approach is that the adoptive transfer of labelled neutrophils alters the neutrophil count in the recipient mouse significantly.[45]

The dynamics of the neutrophil response in the peripheral circulation was different from that in the ischaemic territory. Significantly increased levels of circulating neutrophil were detected at 0.5 h after reperfusion, which was likely due to a rapid egress of neutrophils from the bone marrow reserve into the circulation.[41] However, a similar extent of neutrophil mobilization was also observed in sham-operated animals indicating that the effect on circulating neutrophils is mainly due to surgery and not to ischaemia. In contrast, the growing ischaemic lesion did not seem to (further) mobilize neutrophils within the circulation, which returned to baseline within 24 h after reperfusion, at which high levels of neutrophils were detected in the ischaemic brain region.

To our surprise, we detected fluorescence signals in tMCAO and sham-operated mice after adoptive transfer of LIPO-6S-IDCC-labelled neutrophils on the extracranial ipsilateral regions. Immunohistochemistry demonstrated accumulation of neutrophils in the temporal muscles. The tMCAO model requires ligation of the ECA and thereby restricts perfusion to the extracerebral ECA territory. For rats, the tMCAO procedure has been reported to cause tissue damage in muscles of the ECA territory (including muscles for mastication and swallowing) with negative consequences on outcome.[46] It is conceivable that ECA ligation has also functional implications in the widely used tMCAO mouse model. However, to our knowledge, this has not yet been investigated. Beside functional implications, neutrophil accumulation in the ipsilateral muscle might have also affected quantification of fluorescence signals. ROIs were drawn carefully to measure only over the brain regions excluding extracerebral tissue (Figure 4(a)). In sham-operated animals, the normalized fluorescence intensities was found to be about 10% higher over the ipsilateral hemisphere compared with the contralateral side, despite no detectable neutrophil accumulation in the brain. This indicates that there is spillover from fluorescence of labelled neutrophils from the ipsilateral muscle into the brain region.

During inflammation, circulating neutrophils are recruited from the vessels via rolling, arrest and diapedesis, guided by endothelial adhesion molecules and chemokines.[4] However, if mediators of the multistep adhesion cascade regulate neutrophil recruitment at the cerebral vasculature following transient ischaemia is hitherto unknown. We have used NIRF imaging to study the role of α4-integrins that has been implicated in neutrophil arrest to the endothelium,[4] but is also expressed on other leukocyte subpopulations.[15] We observed a significant reduction in normalized fluorescence intensities in mice that received an antibody against α4-integrin at 18 and 24 h after reperfusion compared with control, while at 48 h, no differences between the groups was detected. Immunohistochemistry, though performed in only a few animals, confirmed our NIRF data at 48 h after reperfusion. However, we did not investigate earlier time points. This findings support a role of VLA-4 with any of its endothelial ligands, VCAM-1, fibronectin or JAM-B in mediating neutrophil trafficking to the brain after cerebral ischaemia.

The neutrophil response clearly occurs during the acute stage when substantial secondary lesion growth

occurs.[30] With immunohistochemistry, we found only low numbers of neutrophils around the ischaemic lesion. Recent studies indicate that these neutrophils do not infiltrate the brain parenchyma, but rather remain restricted to luminal surfaces or perivascular spaces of cerebral vessels including the leptomeninges.[32,34] Neutrophils might still exert their deleterious action via interaction with the vasculature. It has been shown that neutrophils can release cytokines, proteases and reactive oxygen species during an oxidative burst and are involved in microvascular disturbances,[47] and blood–brain barrier damage.[12] In addition, neutrophils might contribute to secondary thrombus formation after cerebral ischaemia as they interact with platelets, participate in fibrin cross-linkage and trigger thrombin activation by inducing the extrinsic tissue factor/FVIIa pathway.[14] In our study, blocking of α4-integrin led to a reduction of the ischaemic lesion at 48 h after reperfusion. Anti-α4-integrin antibody-mediated treatment, has so far yielded contradictory results for its neuroprotective effects following cerebral ischaemia in rodents. While several previous studies have demonstrated a reduction of the ischaemic damage and improved functional deficits after that anti-α4-integrin antibody treatment,[19,15,48,49] two studies reported no effect of treatment on the ischaemic lesion.[50,51] The difference in the neuroprotective efficacy might be attributed to different batches of antibodies used, or differences in housing and experimental conditions that might affect the inflammatory response following cerebral ischaemia.[52,53] However, we also calculated the group size according to normalized fluorescence intensities as a primary end point. For the cerebral lesion, the present study was underpowered (power = 0.67). Preclinical multi-centre studies are more suited to address this question and to conduct treatment studies with sufficient statistical power. Indeed, such a trial with large pooled data samples demonstrated that anti-α4-integrin antibody did not reduce lesion size after filament tMCAO in the mouse.[51]

In future studies, we want to refine our current approach and use molecular probes that can directly visualize neutrophils function to elucidate how neutrophils partake in ischemic tissue injury. NIRF imaging might constitutes an attractive tool to study the neutrophil response in experimental models of cerebral ischaemia and potentially in other inflammatory diseases.

Funding

The author(s) disclosed receipt of the following financial support for the research, authorship, and/or publication of this article: Swiss National Science Foundation (Grant PZ00P3_136822) and the Hartmann-Müller Foundation to JK and the Swiss Heart Foundation to GE and BE.

Acknowledgements

The authors are grateful for excellent technical support from the technical staff in the Histology Laboratory, Laboratory for Animal Model Pathology, University of Zurich. They also thank Ramanil Perera (Institute for Biomedical Engineering, ETH & University of Zurich) for supporting histology and microscopy. All raw data are available at www.figshare.com within the project 'Neutrophil tracking in cerebral ischemia' with the DOI 10.6084/m9.figshare.4052322.

Declaration of conflicting interests

The author(s) declared no potential conflicts of interest with respect to the research, authorship, and/or publication of this article.

Authors' contributions

MV, BE and JK conceived and designed the experiments. MV, GE, TP, US, AK and JK performed the experiments. MV, GE, TP, US, AK and JK analysed the data. MV, GE, AK, JR, MR, BE and JK interpreted results. KL contributed reagents and materials. MV, GE and JK wrote the article. All coauthors made critical revisions to the manuscript.

Supplementary material

Supplementary material for this paper can be found at http://jcbfm.sagepub.com/content/by/supplemental-data

References

1. Endres M, Engelhardt B, Koistinaho J, et al. Improving outcome after stroke: overcoming the translational roadblock. *Cerebrovasc Dis* 2008; 25: 268–278.
2. Zhang RL, Chopp M, Chen H, et al. Temporal profile of ischemic tissue damage, neutrophil response, and vascular plugging following permanent and transient (2H) middle cerebral artery occlusion in the rat. *J Neurol Sci* 1994; 125: 3–10.
3. Dereski MO, Chopp M, Knight RA, et al. Focal cerebral ischemia in the rat: temporal profile of neutrophil responses. *Neurosci Res Commun* 1992; 11: 179–186.
4. Ley K, Laudanna C, Cybulsky MI, et al. Getting to the site of inflammation: the leukocyte adhesion cascade updated. *Nat Rev Immunol* 2007; 7: 678–689.
5. Matsuo Y, Onodera H, Shiga Y, et al. Correlation between myeloperoxidase-quantified neutrophil accumulation and ischemic brain injury in the rat. *Stroke* 1994; 25: 1469–1475.
6. Zhang RL, Chopp M, Jiang N, et al. Anti-intracellular adhesion molecule-1 antibody reduces ischemic cell damage after transient but not permanent middle cerebral artery occlusion in the Wistar rat. *Stroke* 1995; 26: 1438–1443.
7. Bednar MM, Raymond S, McAuliffe T, et al. The role of neutrophils and platelets in a rabbit model of thromboembolic stroke. *Stroke* 1991; 22: 44–50.
8. Chen H, Chopp M and Bodzin G. Neutropenia reduces the volume of cerebral infarct after transient middle cerebral artery occlusion in the rat. *Neurosci Res Commun* 1992; 11: 93–99.

9. Enlimomab Acute Stroke Trial Investigators. Use of anti-ICAM-1 therapy in ischemic stroke: results of the Enlimomab Acute Stroke Trial. *Neurology* 2001; 57: 1428–1434.
10. Krams M, Lees KR, Hacke W, et al. Acute Stroke Therapy by Inhibition of Neutrophils (ASTIN): an adaptive dose-response study of UK-279,276 in acute ischemic stroke. *Stroke* 2003; 34: 2543–2548.
11. Berton G, Yan SR, Fumagalli L, et al. Neutrophil activation by adhesion: mechanisms and pathophysiological implications. *Int J Clin Lab Res* 1996; 26: 160–177.
12. Gidday JM, Gasche YG, Copin JC, et al. Leukocyte-derived matrix metalloproteinase-9 mediates blood-brain barrier breakdown and is proinflammatory after transient focal cerebral ischemia. *Am J Physiol Heart Circ Physiol* 2005; 289: H558–H568.
13. Allen C, Thornton P, Denes A, et al. Neutrophil cerebrovascular transmigration triggers rapid neurotoxicity through release of proteases associated with decondensed DNA. *J Immunol* 2012; 189: 381–392.
14. De Meyer SF, Denorme F, Langhauser F, et al. Thromboinflammation in stroke brain damage. *Stroke* 2016; 47: 1165–1172.
15. Liesz A, Zhou W, Mracskó É, et al. Inhibition of lymphocyte trafficking shields the brain against deleterious neuroinflammation after stroke. *Brain* 2011; 134: 704–720.
16. Stephens-Romero SD, Mednick AJ and Feldmesser M. The pathogenesis of fatal outcome in murine pulmonary aspergillosis depends on the neutrophil depletion strategy. *Infect Immun* 2005; 73: 114–125.
17. Jaeger BN, Donadieu J, Cognet C, et al. Neutrophil depletion impairs natural killer cell maturation, function, and homeostasis. *J Exp Med* 2012; 209: 565–580.
18. Hasenberg A, Hasenberg M, Männ L, et al. Catchup: a mouse model for imaging-based tracking and modulation of neutrophil granulocytes. *Nat Methods* 2015; 12: 445–452.
19. Neumann J, Riek-Burchardt M, Herz J, et al. Very-late-antigen-4 (VLA-4)-mediated brain invasion by neutrophils leads to interactions with microglia, increased ischemic injury and impaired behavior in experimental stroke. *Acta Neuropathol* 2015; 129: 259–277.
20. Holtmaat A, Bonhoeffer T, Chow DK, et al. Long-term, high resolution imaging in the mouse neocortex through a chronic cranial window. *Nat Protoc* 2009; 4: 1128–1144.
21. Wunder A and Klohs J. Optical imaging of vascular pathophysiology. *Basic Res Cardiol* 2008; 103: 182–190.
22. Klohs J, Steinbrink J, Nierhaus T, et al. Noninvasive near-infrared imaging of fluorochromes within the brain of live mice: an in vivo phantom study. *Mol Imaging* 2006; 5: 180–187.
23. Bourayou R, Boeth H, Benav H, et al. Fluorescence tomography technique optimized for noninvasive imaging of the mouse brain. *J Biomed Opt* 2008; 13: 041311.
24. Klohs J, Gräfe M, Graf K, et al. In vivo imaging of the inflammatory receptor CD40 after cerebral ischemia using a fluorescent antibody. *Stroke* 2008; 39: 2845–2852.
25. Klohs J, Steinbrink J, Bourayou R, et al. Near-infrared fluorescence imaging with fluorescently labeled albumin: a novel method for non-invasive optical imaging of blood-brain barrier impairment after focal cerebral ischemia in mice. *J Neurosci Methods* 2009; 180: 126–132.
26. Klohs J, Baeva N, Steinbrink J, et al. In vivo near-infrared fluorescence imaging of matrix metalloproteinase activity after cerebral ischemia. *J Cereb Blood Flow Metab* 2009; 29: 1284–1292.
27. Kim DE, Kim JY, Nahrendorf M, et al. Direct thrombus imaging as a means to control the variability of mouse embolic infarct models: the role of optical molecular imaging. *Stroke* 2011; 42: 3566–3573.
28. Bahmani P, Schellenberger E, Klohs J, et al. Visualization of cell death in mice with focal cerebral ischemia using fluorescent annexin A5, propidium iodide, and TUNEL staining. *J Cereb Blood Flow Metab* 2011; 31: 1311–1320.
29. Barber PA, Rushforth D, Agrawal S, et al. Infrared optical imaging of matrix metalloproteinases (MMPs) up regulation following ischemia reperfusion is ameliorated by hypothermia. *BMC Neurosci* 2012; 13: 76.
30. Hata R, Maeda K, Hermann D, et al. Evolution of brain infarction after transient focal cerebral ischemia in mice. *J Cereb Blood Flow Metab* 2000; 20: 937–946.
31. Stuker F, Baltes C, Dikaiou K, et al. Hybrid small animal imaging system combining magnetic resonance imaging with fluorescence tomography using single photon avalanche diode detectors. *IEEE Trans Med Imaging* 2011; 30: 1265–1273.
32. Enzmann G, Mysiorek C, Gorina R, et al. The neurovascular unit as a selective barrier to polymorphonuclear granulocyte (PMN) infiltration into the brain after ischemic injury. *Acta Neuropathol* 2013; 125: 395–412.
33. McColl BW, Carswell HV, McCulloch J, et al. Extension of cerebral hypoperfusion and ischaemic pathology beyond MCA territory after intraluminal filament occlusion in C57BL/6J mice. *Brain Res* 2004; 997: 15–23.
34. Perez-de-Puig I, Miró-Mur F, Ferrer-Ferrer M, et al. Neutrophil recruitment to the brain in mouse and human ischemic stroke. *Acta Neuropathol* 2015; 129: 239–257.
35. Vajkoczy P, Laschinger M and Engelhardt B. Alpha4-integrin-VCAM-1 binding mediates G protein-independent capture of encephalitogenic T cell blasts to CNS white matter microvessels. *J Clin Invest* 2001; 108: 557–565.
36. Boxio R, Bossenmeyer-Pourie C, Steinckwich N, et al. Mouse bone marrow contains large numbers of functionally competent neutrophils. *J Leukoc Biol* 2004; 75: 604–611.
37. Ivetic A and Ridley AJ. The telling tail of L-selectin. *Biochem Soc Transact* 2004; 32: 1118–1121.
38. Jones DH, Anderson DC, Burr BL, et al. Quantitation of intracellular Mac-1 (CD11b/CD18) pools in human neutrophils. *J Leukoc Biol* 1988; 44: 535–544.
39. Lacal P, Pulido R, Sánchez-Madrid F, et al. Intracellular localization of a leukocyte adhesion glycoprotein family in the tertiary granules of human neutrophils. *Biochem Biophys Res Commun* 1988; 154: 641–647.

40. Gelderblom M, Leypoldt F, Steinbach K, et al. Temporal and spatial dynamics of cerebral immune cell accumulation in stroke. *Stroke* 2009; 40: 1849–1857.
41. Furze RC and Rankin SM. Neutrophil mobilization and clearance in the bone marrow. *Immunology* 2008; 125: 281–288.
42. Stevens SL, Bao J, Hollis J, et al. The use of flow cytometry to evaluate temporal changes in inflammatory cells following focal cerebral ischemia in mice. *Brain Res* 2002; 932: 110–119.
43. Lord BI, Molineux G, Pojda Z, et al. Myeloid cell kinetics in mice treated with recombinant interleukin-3, granulocyte colony-stimulating factor (CSF), or granulocyte-macrophage CSF in vivo. *Blood* 1991; 77: 2154–2159.
44. Coxon A, Tang T and Mayadas TN. Cytokine-activated endothelial cells delay neutrophil apoptosis in vitro and in vivo. A role for granulocyte/macrophage colony-stimulating factor. *J Exp Med* 1999; 190: 923–934.
45. Peters LL, Cheever EM, Ellis HR, et al. Large-scale, high-throughput screening for coagulation and hematologic phenotypes in mice. *Physiol Genomics* 2002; 11: 185–193.
46. Dittmar M, Spruss T, Schuierer G, et al. External carotid artery territory ischemia impairs outcome in the endovascular filament model of middle cerebral artery occlusion in rats. *Stroke* 2003; 34: 2252–2257.
47. del Zoppo GJ, Schmid-Schönbein GW, Mori E, et al. Polymorphonuclear leukocytes occlude capillaries following middle cerebral artery occlusion and reperfusion in baboons. *Stroke* 1991; 22: 1276–1283.
48. Becker K, Kindrick D, Relton J, et al. Antibody to the a4 integrin decreases infarct size in transient focal cerebral ischemia in rats. *Stroke* 2001; 32: 206–211.
49. Relton JK, Sloan KE, Frew EM, et al. Inhibition of a4 integrin protects against transient focal cerebral ischemia in normotensive and hypertensive rats. *Stroke* 2001; 32: 199–205.
50. Langhauser F, Kraft P, Göb E, et al. Blocking of a4 integrin does not protect from acute ischemic stroke in mice. *Stroke* 2014; 45: 1799–1806.
51. Llovera G, Hofmann K, Roth S, et al. Results of a preclinical randomized controlled multicenter trial (pRCT): Anti-CD49d treatment for acute brain ischemia. *Sci Transl Med* 2015; 7: 299ra121.
52. Zhou W, Liesz A, Bauer H, et al. Postischemic brain infiltration of leukocyte subpopulations differs among murine permanent and transient focal cerebral ischemia models. *Brain Pathol* 2013; 23: 34–44.
53. Benakis C, Brea D, Caballero S, et al. Commensal microbiota affects ischemic stroke outcome by regulating intestinal γδ T cells. *Nat Med* 2016; 22: 516–523.